Water Resources Management (2020) 34:2291–2311
https://doi.org/10.1007/s11269-020-02521-8

Numerical Simulation of the Water Surface Movement with Macroscopic Particles on Movable Beds

Alibek Issakhov[1,2] · Yeldos Zhandaulet[1,2] · Aizhan Abylkassymova[1,2]

Received: 7 November 2019 / Accepted: 24 February 2020/
Published online: 31 May 2020

Abstract
In this paper, on the basis of the three-dimensional Navier-Stokes equation, an incompressible fluid flow has been studied numerically when a dam is broken. In order to simulate this problem, a modification of the standard VOF model was carried out and a combination of Newtonian and non-Newtonian models was used. The flow effect on the transport of solid particles and mobile sediment has been shown. Several experiments were simulated to evaluate the computational model. All the obtained numerical results showed good agreement with the experimental data and the results of other authors. The effect of the mixture, which consists of solid particles and mobile deposits on the fluid flow, was studied in detail. The results of the flow behavior and transfer of solid particles at different heights of the moving layer were also shown. According to the numerical results analysis, the effect of dam destruction can be divided into the stage of high-speed impact and the flood stage. The first can cause damage due to instant exposure, and the second can cause damage due to stagnation. The simulation analysis of this work can be useful in hydropower to prevent breakthroughs of reservoirs with real terrain and real coastal contours. This investigation improves the understanding of bed topography with the solid particles effects of downstream dams impact based on simulation analysis.

Keywords Dam breaks modeling · DPM and MPM models · Macroscopic particle interaction · Mud flow · Non-Newtonian fluid

1 Introduction

The floods and dam destruction is an urgent problem in the modern world. This phenomenon is the main topic of study in the field of hydrodynamics and hydraulic engineering due to the

✉ Alibek Issakhov
alibek.issakhov@gmail.com

[1] al-Farabi Kazakh National University, Almaty, Republic of Kazakhstan

[2] Kazakh British Technical University, Almaty, Republic of Kazakhstan

high degree of danger to nearby cities and their population. As in the whole world and in Kazakhstan, this issue is especially acute, since in the past there have already been many victims. Currently, potential catastrophic floods resulting from the dam destruction are of great concern, as they cause great damage. Proof of this is already occurred accidents. In 2010, a dam broke on the Fuhe River in Jiangxi Province in eastern China due to heavy rains. One way or another, 29 million people were affected by the disaster. In the same year, a dam broke on the Indus River in southern Pakistan. Destroyed up to 895 thousand houses flooded more than 2 million hectares of agricultural land. More than 1700 people died. A year later, the dam also broke on the Qiantang River near the city of Hangzhou in Zhejiang province in eastern China. A tidal wave of up to 9 m broke through the dam and washed away many people. Also, disasters on the dams, unfortunately, took place in Kazakhstan. One of the striking examples is the floods of the summer of 1921 in Almaty, as well as the breakthrough of a reservoir in the Almaty region in 2010, which entailed catastrophic destruction and casualties.

The dam break is a catastrophic phenomenon associated with many different factors related to both human activities and environmental factors. This phenomenon has high scientific value. The dam model is used to evaluate and validate a number of theories and approaches in both mathematics and physics Wang et al. (2000). In papers Fondelli et al. (2015), Kleefsman et al. (2005), Kocaman (2007), Ozmen-Cagatay and Kocaman (2011), Fraccarollo and Toro (1995), Ferrari et al. (2010) experimentally investigated the initial stage of a dam breaks. In these works, the most simplified case of the water flow movement along a hard, smooth bottom with various forms of obstacles was used. Whereas in papers Marsooli and Wu (2014), Haltas et al. (2016a, b), Issakhov et al. (2018), Issakhov and Imanberdiyeva (2019), the VOF (Volume of Fluid) method was used to construct a two-phase flow model, which gives a rather high degree of accuracy in comparison with experimental data.

The motion of the flow over a fixed impermeable layer has previously been well studied in many of the above works. But with large-scale damage, the transfer of deposits such as stones, sand, debris, etc. is possible. Moreover in the papers Amicarelli et al. (2017), Crespo et al. (2008), Wang et al. (2016), the destruction case of the bottom during the collapse of a huge mass of water has been considered. In many studies, the meshless SPH(Smoothed Particle Hydrodynamics) method was used to model the soil. The experimental dam breaks over a granular earth surface was studied in papers Pontillo (2010), Spinewine (2010). Using this approach, the soil appears as a collection of particles. The fluid flow can be represented in the same way, i.e., the phenomenon of dam breaking can be studied as the collapse of dry particles Amicarelli et al. (2017), Li and Zhao (2018). The SPH method gives good results when studying the motion of a free surface in three-dimensional problems. This was demonstrated in paper Xu (2016). As expected the obtained data demonstrated a good agreement with experimental data in problems with a vertical wall, a cubic and a cylindrical obstacle.

When studying the dam break, the mudflow that makes up a moving stream in most cases does not have a constant viscosity. In addition, sediment transport such as mud, clay, etc. is also possible Coussot (1995). Then, in order to have the dependence of fluid viscosity on stress, it is necessary to use the non-Newtonian fluid model Gotoh and Fredsøe (2000). Such an addition introduces significant differences in the propagation of waves and the motion of the free flow surface Janosi et al. (2004), Lauber and Hager (1998). Consideration of non-Newtonian fluids allows better study of more complex natural flows, such as avalanches, debris flows, mud flows, the movement of various solutions, etc., than the study of exclusively Newtonian fluids, such as water. Dam destruction by pure non-Newtonian fluids, in particular gel and liquid clay, was studied in papers Ancey and Cochard (2009), Chambon et al. (2009),

Boroomand et al. (2007), Movahedi et al. (2018), Hosseinzadeh-Tabrizi and Ghaeini-Hessaroeyeh (2017), Issakhov and Zhandaulet (2020). Even more in paper Lin and Chen (2013) also studied the effect of friction on flow motion by considering the motion and velocity of the leading edge of the flow. Another example of non-Newtonian fluid flow motion can be found in various mixtures in civil striotelism, such as runoff of freshly mixed concrete Saak et al. (2004), Roussel and Coussot (2005), Piau (2006).

A comprehensive study of the non-Newtonian fluid flow allows us to distinguish several main stages of wave propagation: decay, inertia phase and transport phase Hogg and Woods (2001), Hogg and Pritchard (2004). At different points in time, at each of these stages, influence a large number of different physical mechanisms, which must also be taken into account when building the model.

The next step in studying the flow during the dam destruction is taking into account the bursting avalanche does not consist solely of water or some liquid. Then it is necessary to consider the presence of solid particles in the mass of the stream. Traditionally, fluid and particles were considered as one equivalent fluid or as two fluids Pitman and Le (2005). A two-dimensional model of the movement of water and particulate matter was studied in papers (Lube et al. (2005), Balmforth and Kerswell (2005), and three-dimensional models were also considered in papers Li and Zhao (2018), Di Cristo et al. (2010), Ancey and Cochard (2009), Chambon et al. (2009), Minussi and Maciel (2012), Saramito et al. (2013), Ward et al. (2009), Andreini (2012), Ancey et al. (2013), Park et al. (2018), Larocque et al. (2013). In paper Lin and Chen (2013) also demonstrated the effect of particle concentration in a mixture on the total flow rate. The results of this work showed that with a decrease in the number of particles, the flow rate increases, with decrease in the total momentum of the mixture.

In paper Li and Zhao (2018) examined the movement of solid particles in a non-Newtonian fluid flow, and also compared with the water mixture flow with particles, the flow of dry particles and three different pure liquids. Much attention was paid to the interaction of solids with liquids, which plays a very important role in changing the energy and movement of the mixture front.

An important aspect in modeling solid particles is also the interaction between them, and their collisions with various obstacles. Large particles immersed in a fluid stream cannot be represented by point masses. In papers Wadnerkar et al. (2016), Luchini et al. (2015), Chara and Kysela (2018) consider the motion of particles and collisions like particle–particle and particle–wall. The drag force and particle torque were also taken into account.

The numerical model described in this work was tested on four test problems of dam break, and the calculated results were compared with the data obtained in experiments. The simulation was implemented in the ANSYS Fluent. Next, various statements of dam break with the transfer of the moving layer and solid particles have been modeled.

In order to achieve the aim, a range of numerical simulations and numerical algorithm have been conducted using computational fluid dynamics (CFD) (Sections 2 and 3). The physical case under review is a dam break flow laboratory experiment with a three-dimensional inhomogeneous terrain Marsooli and Wu (2014), Ozmen-Cagatay and Kocaman (2011), Kocaman (2007) and the water flow over the moving layer of sediment in the tank Spinewine and Zech (2007), Ran et al. (2015) were considered in Section 4. The results from the experiments are used to validate the quality of the CFD set-up. Once the numerical model was validated, an extra additionally problem was also considered in Section 5, the movement of water through an inhomogeneous terrain with different sediment height and macroscopic particles (stones), and a dam, which has a hole.

2 Material and Methods

2.1 The Mathematical Model

To describe this process, 3D continuity equations and averaged Navier-Stokes equations were used for incompressible flows of two immiscible phases, which can be written in such a vector form Hirt and Nichols (1981), Issakhov and Zhandaulet (2020)

$$\nabla u = 0 \tag{1}$$

$$\frac{\partial u}{\partial t} + (\Delta u)u = \frac{1}{\rho} f + \frac{1}{\rho} f_{si} - \frac{1}{\rho}\nabla p + \frac{1}{\rho}\nabla\left(\mu_{eff}\nabla u\right) \tag{2}$$

$$\frac{\partial \chi}{\partial t} + u_j \frac{\partial \chi}{\partial x_j} = 0 \tag{3}$$

where, u is the flow velocity, t is time, p is pressure, ρ is the density of water, f is the external force of the body, μ is the dynamic viscosity. The considered external force of the body, in this case gravitational forces, so f=ρg, where g is the acceleration of gravity. $f_{si} = \frac{\beta\left(u_{pi} - u_i\right)}{\rho}$, where u_{pi} is the particle velocity, β is a coefficient depending on the fraction of voids. When the void fraction is less than 0.8, the coefficient is derived from the Ergun equation for the densified layer. When the fraction of voids is greater than 0.8, the motion of the particle has a weak effect on the motion of the mass; for this region, the modified equation of fluid resistance for an individual particle has been used.

In incompressible Newtonian fluids, the tensor stress is proportional to the strain rate tensor Gotoh and Fredsøe (2000), Coussot (1995), Ancey and Cochard (2009):

$$\overrightarrow{\tau} = \mu \overrightarrow{D} \tag{4}$$

$$\overrightarrow{D} = \left(\frac{\partial u_j}{\partial x_i} + \frac{\partial u_i}{\partial x_j}\right) \tag{5}$$

μ dynamic viscosity, which is independent of $\overrightarrow{D}$.

For non-Newtonian fluids, the tensor stress is written

$$\overrightarrow{\tau} = \eta\left(\overrightarrow{D}\right)\overrightarrow{D} \tag{6}$$

η is a function of all three invariants of the strain rate tensor $\overrightarrow{D}$. Non-Newtonian flow is modeled in accordance with the following power law for non-Newtonian viscosity

$$\eta = k\gamma^{n-1}H(T) \tag{7}$$

k is a measure of the average viscosity of a liquid (an indicator of consistency);

n is a measure of the deviation of a fluid from Newtonian (power index), γ refers to the second invariant $\overrightarrow{D}$ and is defined as

$$\gamma = \sqrt{{}^{1}/_{2}\overrightarrow{D} : \overrightarrow{D}} \tag{8}$$

H (T) is the temperature dependence, known as the Arrhenius law.

$$H(T) = \exp\left[\alpha\left(\frac{1}{T-T_0} - \frac{1}{T_\alpha - T_0}\right)\right] \tag{9}$$

where α is the ratio of activation energy to the thermodynamic constant and T_α is the temperature of the medium and T_0 is the absolute temperature. The temperature dependence is only enabled when the energy equation is turned on. When setting the parameter toα=0, the temperature dependence is ignored.

The VOF method was first introduced by Hirt and Nichols (1981). The equations for the phases have been solved by introducing the function F, defined as the average value of the phase characteristic function above the cell of the computational grid. Therefore, F represents the volume fraction occupied by the phase in the grid cell. At the end of each time step, the local volume fraction in the cell has been used to calculate the local density and viscosity values needed to solve the Navier-Stokes equations. For "mixed cells" (that is, containing more than one phase), the equivalent density and viscosity have been calculated by linear interpolation based on the volume fraction.

To close the Reynolds-averaged Navier-Stokes (RANS) equations, the k-ω SST turbulent model with two additional partial differential equations for the two variables k and ω has been used.

$$\frac{\partial \rho k}{\partial t} + \frac{\partial \rho u_j k}{\partial x_j} = P_k - \beta^* k\omega + \frac{\partial}{\partial x_j}\left((\mu + \delta^* \mu^*_t)\frac{\partial k}{\partial x_j}\right)$$

$$\frac{\partial \rho \omega}{\partial t} + \frac{\partial \rho u_j \omega}{\partial x_j} = \alpha S^2 - \beta\omega^2 + \frac{\partial}{\partial x_j}\left((\mu + \delta_\omega \mu_t)\frac{\partial \omega}{\partial x_j}\right) + 2(1-f_1)\delta_{\omega_2}\frac{1}{\omega}\frac{\partial k}{\partial x_i}\frac{\partial \omega}{\partial x_i}$$

where

$$\mu_t = \frac{a_1 k}{\max(a_1\omega_1 S f_2)}$$

$$P_{k_1} = \mu_t\left(\frac{\partial u_i}{\partial x_j} + \frac{\partial u_j}{\partial x_i}\right)\frac{\partial u_i}{\partial x_j} - \frac{2}{3}\frac{\partial u_k}{\partial x_k}\left(3\mu_t\frac{\partial u_k}{\partial x_k} + \rho k\right)$$

$$f_2 = \tanh\left(\left(\max\left(\frac{2\sqrt{k}}{\beta^*\omega y}, \frac{500\mu}{y^2\omega}\right)\right)^2\right) \qquad P_k = \min\left(P_{k_1}, 10\beta^* k\omega\right)$$

$$f_1 = \tanh\left(\left(\min\left(\max\left(\frac{\sqrt{k}}{\beta^*\omega y}, \frac{500\mu}{y^2\omega}\right), \frac{4\delta\omega_2 k}{CD_{k\omega}y^2}\right)\right)^4\right)$$

$$CD_{k\omega} = \max\left(2\rho\delta_{\omega_2}\frac{1}{\omega}\frac{\partial k}{\partial x_i}\frac{\partial \omega_i}{\partial x_i}, 10^{-10}\right) \qquad \phi = \phi_1 f_1 + \phi_2(1-f_1)$$

The constants have the following meanings:

$$\alpha_1 = \frac{5}{9} \quad \alpha_2 = 0,44 \quad \beta_1 = \frac{3}{40} \quad \beta_2 = 0,0828$$
$$\beta^* = \frac{9}{100} \quad \delta_{k_1} = 0,85 \quad \delta_{k_2} = 1 \quad \delta_{\omega_1} = 0,5 \quad \delta_{\omega_2} = 0,856$$

2.2 DPM (Discrete Phase Model)

Currently, there are two approaches for the numerical calculation of multiphase flows: the Euler-Lagrange approach and the Euler-Euler approach.

2.2.1 Euler-Lagrange Approach

The used Lagrange model of the discrete phase follows the Euler-Lagrange approach. The liquid phase is considered as continuous by solving the Navier-Stokes equations, while the dispersed phase is solved by tracking a large number of particles through the calculated flow field. The transfer of momentum, mass and energy between the continuous and dispersed phases can occur. This approach is greatly simplified when interactions between particles can be neglected, and this requires that the dispersed second phase occupy a small volume fraction, even if a high mass load is permissible ($m_{particles} \geq m_{fluid}$). Particle trajectories are calculated individually at regular intervals when calculating the continuous phase.

2.3 MPM (Macroscopic Particle Model)

The MPM model simulates the behavior of large (macroscopic) particles and their interaction with fluid flow, walls and other particles. The MPM model is applicable to Lagrangian particle flows that cannot be solved using traditional point mass particle models. In such flows, the particle size cannot be neglected. In these situations, the particle volume should be taken into account when modeling hydrodynamics and collisions. The MPM model provides a special mode that takes into account the following: 1) Flow blocking and impulse transmission; 2) Calculation of resistance and torque on particles; 3) Collision of particles with particles and particles with walls, as well as friction dynamics; 4) Sedimentation and accumulation of particles; 5) The forces of attraction between particles and walls and particles.

3 Numerical Simulation Algorithm

The Reynolds-averaged Navier-Stokes (RANS) Eqs. (1)–(9) have been discretized on a fixed Cartesian grid using the finite volume method. The PISO algorithm (Issa 1986) was chosen as a numerical method for solving the (1)–(Coussot 1995) equations. This is an extension of the SIMPLE algorithm used in computational fluid dynamics to solve the Navier-Stokes equations. PISO is a pressure velocity calculation procedure for the Navier-Stokes equations, originally developed for non-iterative calculation of unsteady compressible flow, but has been successfully adapted to stationary problems. PISO includes one prediction step and two corrector steps and is designed to ensure mass conservation using predictor-corrector steps.

4 Calibration and Verification of the Model

4.1 Test Problem 1. Inhomogeneous Terrain

Further, the developed model has been tested for the water movement through a heterogeneous terrain having a trapezoidal shape. A trapezoidal inhomogeneous shape of the terrain was chosen, since when water hits an inhomogeneous relief, the pressure distribution along the walls shows the minimum value, which is the most optimal form Issakhov et al. (2018).

The obtained numerical results during the solution were compared with the data from the measurement presented in Kocaman (2007), as well as with the data from the computation obtained by Marsooli and Wu (2014) and Ozmen-Cagatay and Kocaman (2011) under the same conditions. These parameters can be described as: to design the simulation region. Moreover the 3D-dimensional coordinate system was represented, the center of which is displayed in Fig. 1. The gravity force effects in the opposite direction to the y axis. The measurement was performed in the tank with the horizontal location, the length of which is along the axis x = 903 cm, along the axis y = 34 cm and along the axis z = 30 cm. The gate holding the volume of water was normal to the axis x and lies at a distance x = 465 cm. The initial water height was h0 = 25 cm. The non-uniform terrain height was 7.5 cm. The length along the z axis was 30 cm. The ledge normal section to the z axis and its sizes, the 3D tank diagram are displayed in Fig. 1. The 3D scheme of the tank is also illustrated in Fig. 1. The edges of the tank, positioned at x = 903 cm and y = 34 cm would be taken as open, all others faces - impenetrable walls.

For computational modeling, a uniform computational mesh consisting of 922,080 hexagonal elements was used. The computational cells size was 1 cm.

Figure 2 illustrates the obtained computational data of changes in the water level for various times, where h is the height of the water level, and their comparison with data from the measurement Kocaman (2007) and simulation results by other authors Marsooli and Wu (2014); Ozmen-Cagatay and Kocaman (2011). The values presented in the graphs were dimensionless using the initial height of the main volume of water (h0). Moreover Fig. 3 displays the 2D and 3D changes in the water interface during the dam break for various times (t = 1.9 s, t = 2.8 s, t = 3.3 s, t = 3.68 s, t = 4.74 s, t = 6.68 s).

In this paper, just like in the paper Marsooli and Wu (2014), the LES model of turbulence was used, whereas in the paper Ozmen-Cagatay and Kocaman (2011), the k–ε turbulent model averaged over the depth by two-dimensional and three-dimensional models with cell size equal to 0.5 cm.

From Fig. 2, it can be noted that the obtained computational values in this work and the results that were obtained in the paper Marsooli and Wu (2014) using the turbulent LES model display the best values close to the measured values than the obtained values in paper Ozmen-Cagatay and Kocaman (2011) using the k–ε turbulent model. Also from Fig. 2 it can be concluded that at t = 1.9 s, the moving water column covers the non-uniform terrain completely, and at t = 2.8 s, the struck part of the water around the relief goes back, forming an inversely wave. It may also be noticed from the graph that at t = 1.9, 2.8 and 6.68 s, the received numerical data of the water interface are smooth and the simulated data are as close as possible to the measured values Kocaman (2007) than the computational values of other authors Marsooli and Wu (2014); Ozmen-Cagatay and Kocaman (2011). As it can be seen, at t = 3.3 and 3.68 s, smallest waves form on the water surface, this kind of waves form vortices and the water surface comes restless, since the striking part of the water on the inhomogeneous

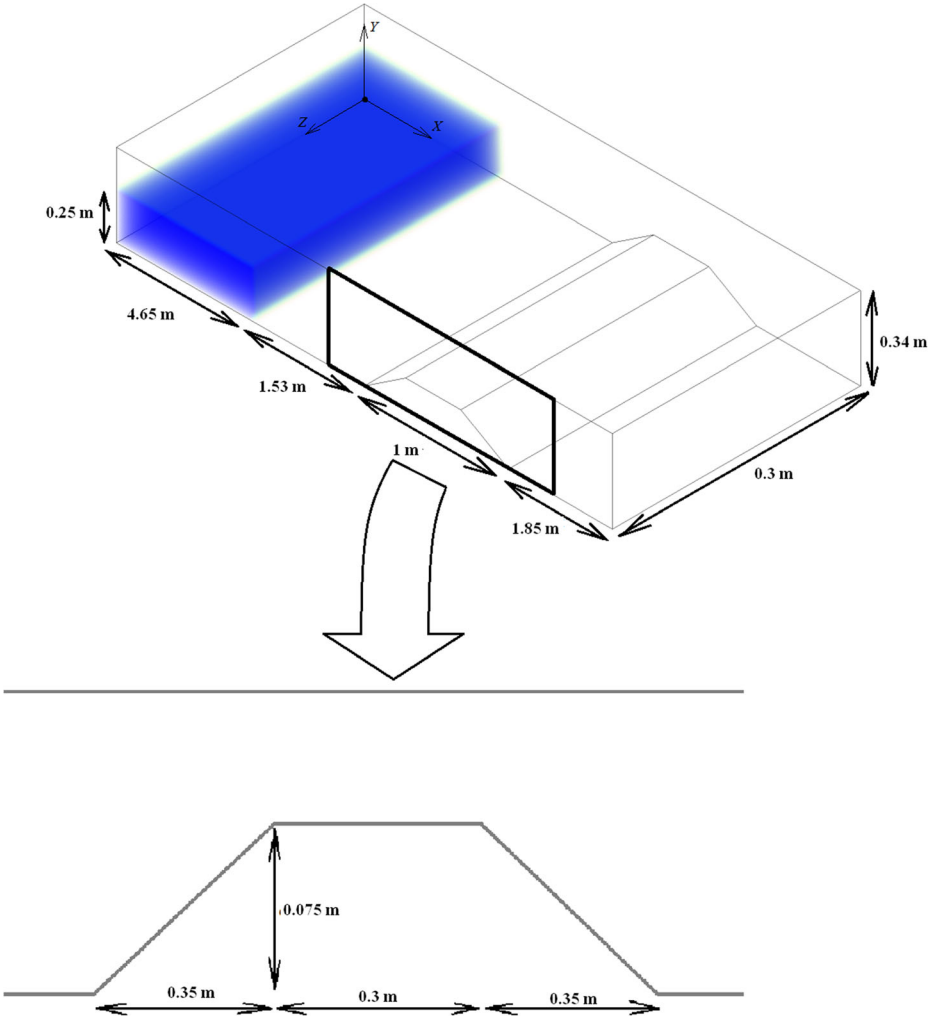

Fig. 1 The 3D-dimensional diagram of a reservoir with a heterogeneous topography and a diagram of the step itself in section

relief creates a reverse wave, this reverse wave is collides with the going wave. This physical phenomenon leads to slight discrepancies in the obtained results with measured values Kocaman (2007). In general, from the graphs it could be observed that the obtained computational values, the used turbulent model give very well agreement with the measured values Kocaman (2007).

As could be seen, at t = 3.3 s and t = 3.68 s, small waves form on the surface of the water, these waves form vortices and the surface of the water becomes unstable (Fig. 3), since the impacted part of the water on the inhomogeneous relief creates a backward wave, this return wave collides with a traveling wave. This physical phenomenon leads to small discrepancies between the obtained data and experimental data Kocaman (2007). In general, it could be seen from the graphs that the obtained data from the computations and the used turbulent model give appreciate agreement with the data from the measurement Kocaman (2007).

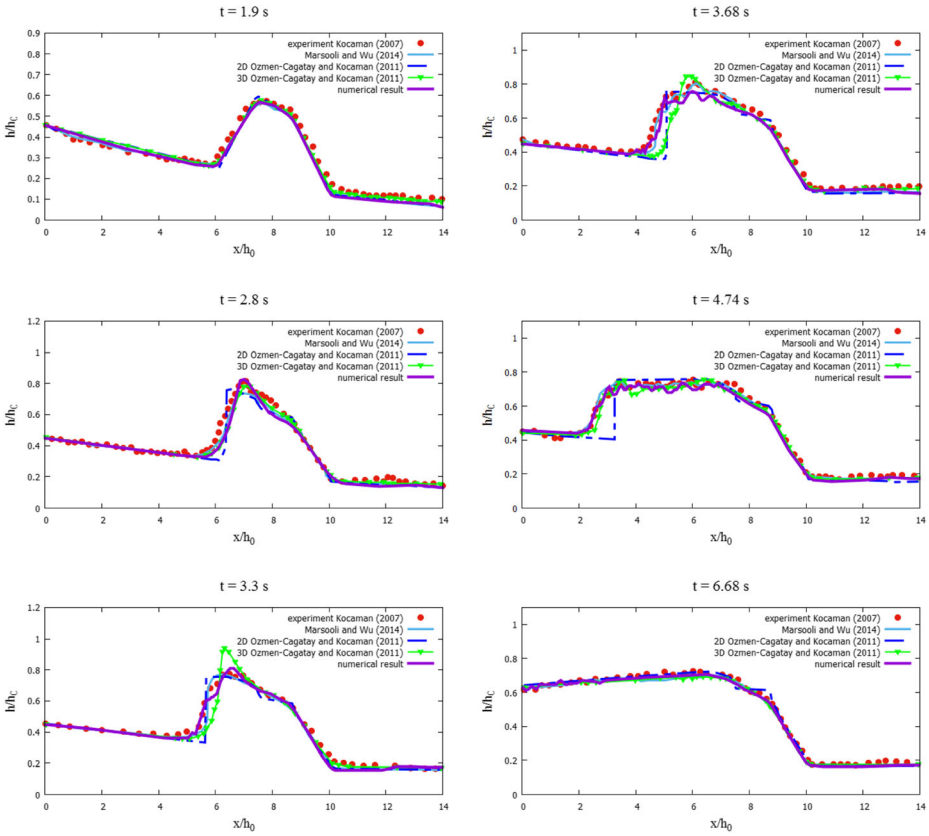

Fig. 2 Change in water level altitude when a dam breaks for various times. (t = 1.9 s, t = 2.8 s, t = 3.3 s, t = 3.68 s, t = 4.74 s, t = 6.68 s)

4.2 Test Problem 2. The Water Flow over the Moving Layer of Sediment in the Tank

In order to verify the proposed model, in this section the control test of the flow of the dam break over the mobile layer of sediment have been applied. A laboratory experiment Spinewine and Zech (2007) includes a water tank separated in the middle by a shutter, and the bottom of the tank is covered with a layer of moving deposits. The experimental area has a height of 0.7 m and a total length of 6 m, i.e. 3 m on both sides of the central gate, imitating an idealized dam. The channel width was set equal to 0.25 m along the entire length of the channel. The water depth of this experiment is 0.35 m as shown in Fig. 4. In this natural measurement, homogeneous coarse sand with a density of 2683 kg/m^3 and polyvinyl chloride with a density of 1580 kg/ m^3 were used as the lower layer. In our model, the sediment phase has been considered as a non-Newtonian fluid. For a non-Newtonian fluid, the effective viscosity has been computed using Eq. (6).

From the modeling photographs in Fig. 5, it can be seen that a significant amount of precipitation had been destroyed by the flow of the dam break. Which in turn leads to ablation of sediments, changing the depth of the stream. Ultimately, in the viscous phase, the flow becomes dominant and slows down by friction. Due to the presence of coarse

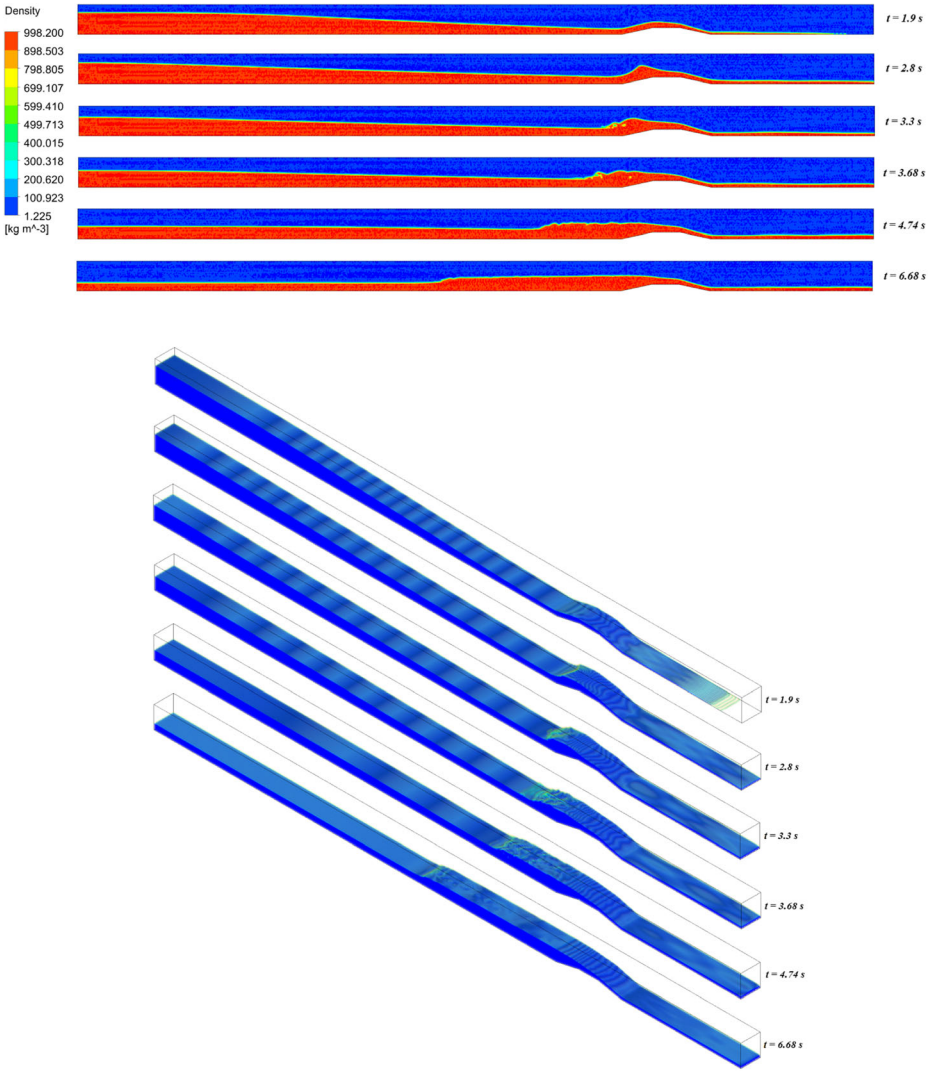

Fig. 3 The 2D-dimensional and 3D-dimensional change in the water interface during the dam break for various times (t = 1.9 s, t = 2.8 s, t = 3.3 s, t = 3.68 s, t = 4.74 s, t = 6.68 s)

sand, the flow slows down during breakthrough and leads to sediment transport and decreases. The proposed model has been also compared with numerical results Spinewine and Zech (2007) and experimental data from other authors Spinewine and Zech (2007). Figure 6 shows the simulations and experiments Spinewine and Zech (2007) during the dam break with geomorphological changes at different moments (t = 0.25 s, 0.5 s, 0.75 s, 1.0 s). Comparisons in Fig. 6 showed that the calculated free surface profiles are in fairly good agreement with data from the experiment Spinewine and Zech (2007) and computational data from other authors Ran et al. (2015).

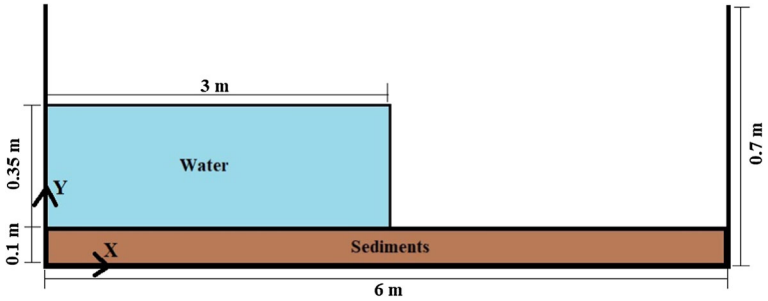

Fig. 4 Geometry and dimensions of the experiment Spinewine and Zech (2007)

In general, the obtained results indicate good agreement between the data from the experiment and computational data, both when modeling changes in water levels and changes in soil levels.

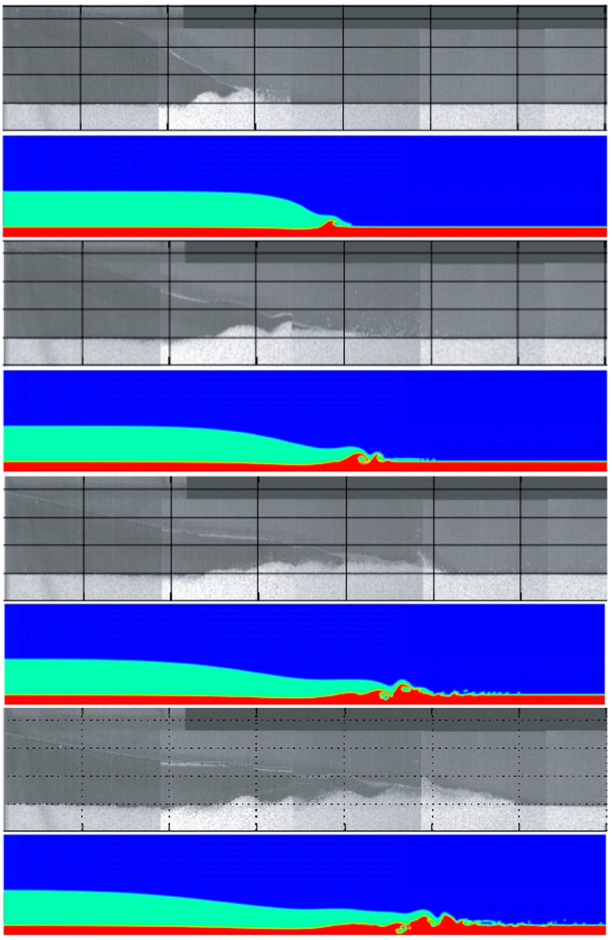

Fig. 5 Pictures of modeling and experiment Spinewine and Zech (2007) of a dam breaking with geomorphological changes at the moments t = 0.25, 0.5, 0.75, 1 s

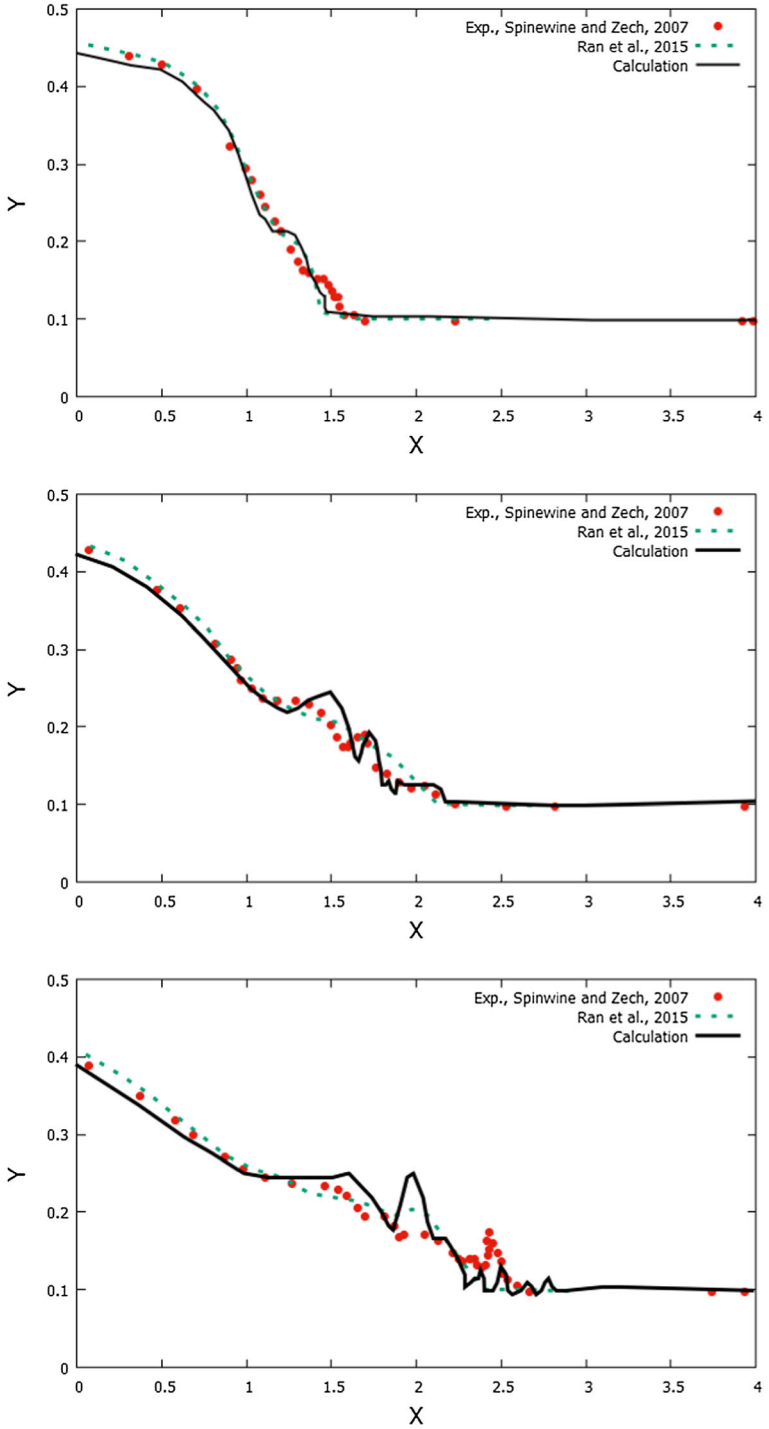

Fig. 6 Comparison of free surface profiles with experimental data Spinewine and Zech (2007) and numerical data from other authors Ran et al. (2015)

5 Modeling the Flow of Newtonian and Non-Newtonian Liquids with Solid Particles (Combined Problem)

This section discusses the combined problem of the water movement with a mixture of macroscopic particles and with a mixture of deposition through a heterogeneous terrain and a dam with a hole. The heterogeneous topography was selected as a solid trapezoidal shape, and there was a hole in the middle of the dam itself. In this problem were combined the heterogeneous topography and a dam with a hole that was used in previous problems. In this problem, to close the systems of the Navier-Stokes equations, the SST k-ω turbulent model was also used tested with the data from experiment for this class of problems. It could be noticed that the used SST k-ω turbulent model for all test cases displayed good agreement with data from experiment and data from computation of other authors. In this case, the water movement with a mixture of macroscopic particles and different heights of the sediments mixture using an inhomogeneous terrain and a dam with a hole has been studied; this problem is closest to the real conditions when breaking the dam. The behavior and influence of water flow, changes in the distribution of pressure on an obstacle in the presence of particles and with different heights of deposits have been studied. The obtained data as a result of the calculation have been compared with the results of the calculation in the paper (Issakhov and Imanberdiyeva 2019), carried out with similar parameters, but without the use of macroscopic particles and deposits.

As in all previous test cases, a 3D coordinate system was presented to construct the computational mesh, the center of which is illustrated in Fig. 7. The gravitational force acts in the opposite direction to the y axis.

A three-dimensional sketch, which shows all the dimensions of the reservoir, the size of the obstacle, the location of macroscopic particles and sediment, as well as the position of the volume of water in a heterogeneous terrain, are shown in Fig. 7.

Numerical modeling was performed in a horizontal tank, the length of which was along the $x = 1018$ cm axis, along the $y = 34$ cm axis, and along the $z = 30$ cm axis. The water holding volume, the dam, was perpendicular to the x axis and was positioned at a distance $x = 465$ cm from the left parts of the tank. The initial height of the water was 25 cm. The height of the heterogeneous terrain had a continuous trapezoidal shape, which was equal to 7.5 cm. The length along the z axis was 30 cm. The step section, perpendicular to the z axis, and its dimensions are illustrated in Fig. 7. A dam with an opening consists of two symmetrical impermeable walls, they were perpendicular to the x axis and are positioned at a distance $x = 100$ cm from the heterogeneous terrain with a continuous trapezoidal shape. The distance between the walls was 0.4 m. As in the test problem, the thickness of the gate was taken as 1 mm, which is also quite small in comparison with the dimensions of the tank. The macroscopic particles were located right in the middle between the column of water and the heterogeneous topography. The tank face located at $y = 34$ cm was taken as open, all other faces were impermeable walls. The location of the deposition mixture was between the trapezoidal shape of the terrain and the dam, in which there was a hole in the middle. For this simulation, homogeneous coarse sand with a density of 2683 kg/m^3 and polyvinyl chloride with a density of 1580 kg/m^3 were used as the lower layer. For modeling, the sediment phase was considered as a non-Newtonian fluid. For a non-Newtonian fluid, the effective viscosity was computed using Eq. (6). Three variants of modifying a problem with a height of 1 cm, 2 cm, and 4 cm were investigated. A uniform unstructured computational grid was used in the calculations. The size of the tetrahedral cells was 20 mm. The grid contained 1,122,287

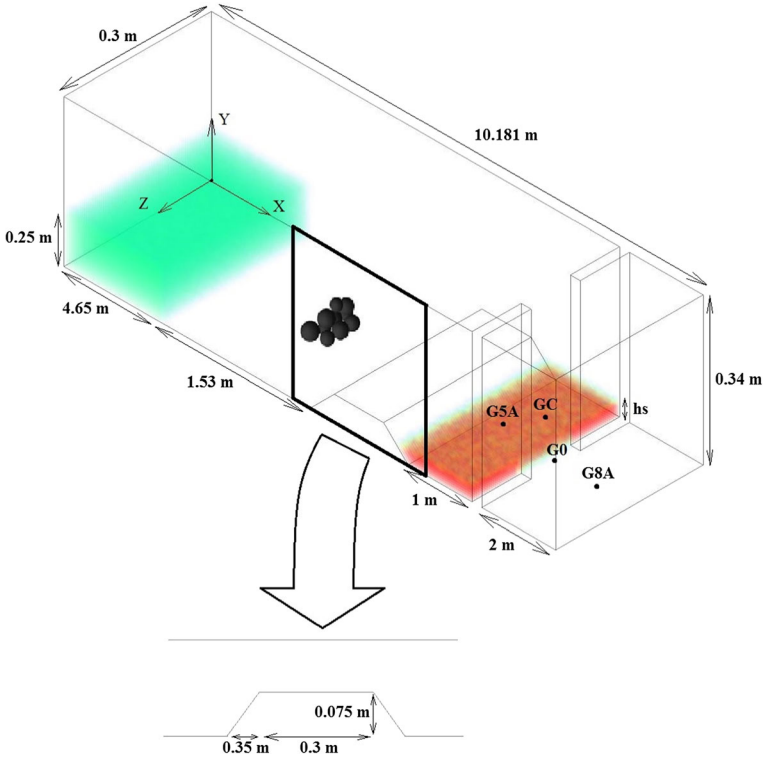

Fig. 7 Combined study area

elements. Particle modeling was performed using the Discrete Phase (DPM) and the Macroscopic Particle Model (MPM) described earlier. Particles were spheres consisting of calcium carbonate (CaCO3) having a density of 2800 kg/m^3. Table 1 shows the coordinates and particle sizes.

Figure 8 shows the change in water level at the control points (G5A, GC, G0, G8A) when a dam is broken for various times with a mixture of macroscopic particles and with a mixture of sediment. Figure 9 displays the change in the wave profile during the dam break for various times (t = 1.7 s, t = 1.9 s, t = 2.8 s, t = 3.3 s, t = 3.68 s, t = 4.74 s, t = 6.68 s) with a mixture of macroscopic particles and with a mixture of sediment. Figure 10a, d, g show 2D changes in the water interface during the dam break for various times (t = 1.7 s, t = 1.9 s, t = 2.8 s, t = 3.3 s, t = 3.68 s, t = 4.74 s, t = 6.68 s) with a mixture of macroscopic particles at various heights of the deposition mixture (hs = 1 cm, 2 cm, 4 cm). Figure 10b, c, e, f, h, i show 3D changes in the water interface during the dam break for various times (t = 1.7 s, t = 1.9 s, t = 2.8 s, t = 3.3 s, t = 3.68 s, t = 4.74 s, t = 6.68 s) with a mixture of macroscopic particles at various heights of the deposition mixture (hs = 1 cm, 2 cm, 4 cm).

Moreover Fig. 8 shows the changes in water level over time at control points and a comparison of the results with obtained data in a similar problem, but without particles Issakhov and Imanberdiyeva (2019). It can be seen that in both cases the flow behavior is similar, however, the presence of macroscopic particles and the deposition mixture causes a large number of height fluctuations in profiles, compared with profiles obtained by the

Table 1 The coordinates of the centers of particles in space and their diameters

Particle Number	Diameter d, m	X, m	Y, m	Z, m
0	0.04	5,395	0,02	0,197
1	0.027	5,4015	0,0135	0,1635
2	0.035	5,3975	0,0175	0,1325
3	0.03	5,4	0,015	0,1
4	0.0317	5,43085	0,01585	0,18435
5	0.037	5,4335	0,0185	0,15
6	0.033	5,4315	0,0165	0,115
7	0.0383	5,415	0,045	0,17
8	0.034	5,415	0,046	0,115
9	0.0283	5,415	0,0635	0,1415

propagation of pure water. In all the values presented on the graphs, real physical quantities were used.

From this data it could be noticed that after a time t = 1.8 s, some nonsmooth peaks appear in the obtained profiles of the water level contour. These peaks in computational results appear due to the fact that the backward flow from the collision collides with a column of water that goes forward, and some oscillatory solutions appear in the resulting profiles. The appearance of the reverse flow could be explained by the fact that a column of water, having passed through a non-uniform terrain, collides with a second obstacle, a dam with a hole, and since the entire volume of water and the mixture with particles and sediments cannot instantly pass this hole completely, which failed to pass, part of the water and the mixture with particles and sediments begins to move back and already collides with a column of water that went forward. These phenomena could be noticed in Fig. 10.

It is also seen from the obtained data that the level of the water column, taking into account the mixture with particles and sediments, has a higher height and a large number of non-smooth water interfaces compared to the mixture. These changes are due to the fact that a

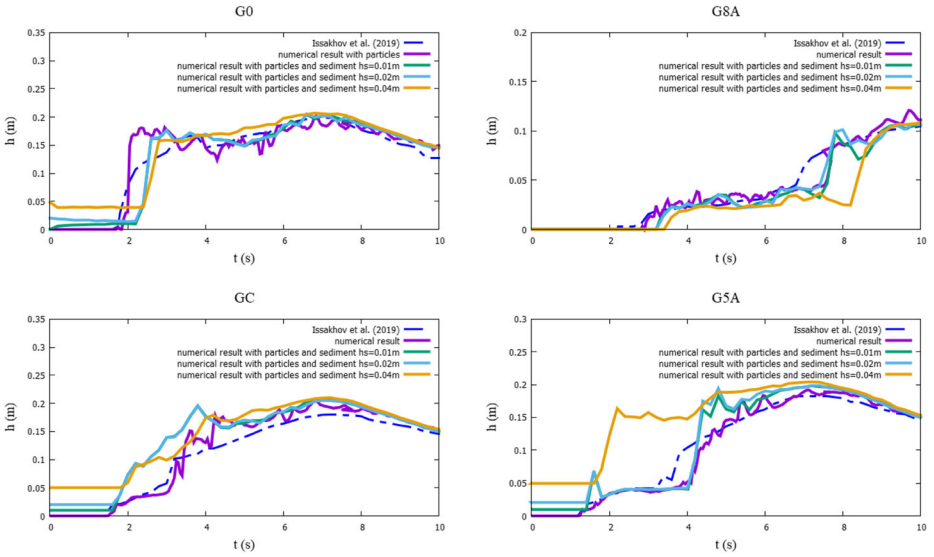

Fig. 8 Change in water level at the control points (G5A, GC, G0, G8A) during the dam break for various times

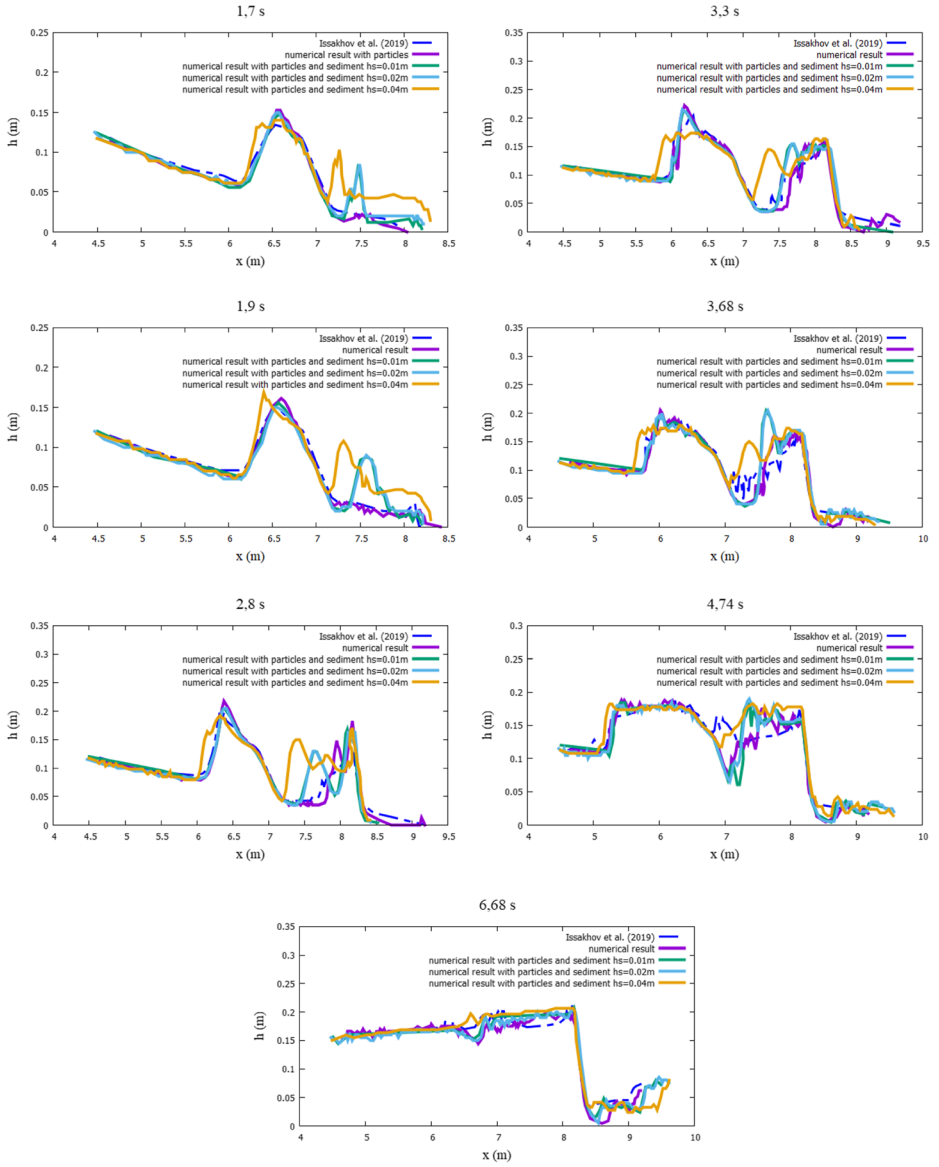

Fig. 9 Change in the wave contour during the dam break for various times. (t = 1.7 s, t = 1.9 s, t = 2.8 s, t = 3.3 s, t = 3.68 s, t = 4.74 s, t = 6.68 s)

column of water, hitting particles, flowing around these particles, creates a water level higher than without particles.

Further, water with particles passes a trapezoidal obstacle, and the amount of precipitation was destroyed by this stream. This in turn leads to ablation of sediments, changing the depth of the stream. Ultimately, in the viscous phase, the flow becomes dominant and slows down by friction. Due to the presence of coarse sand, the flow slows down during breakthrough and leads to sediment transport and decreases.

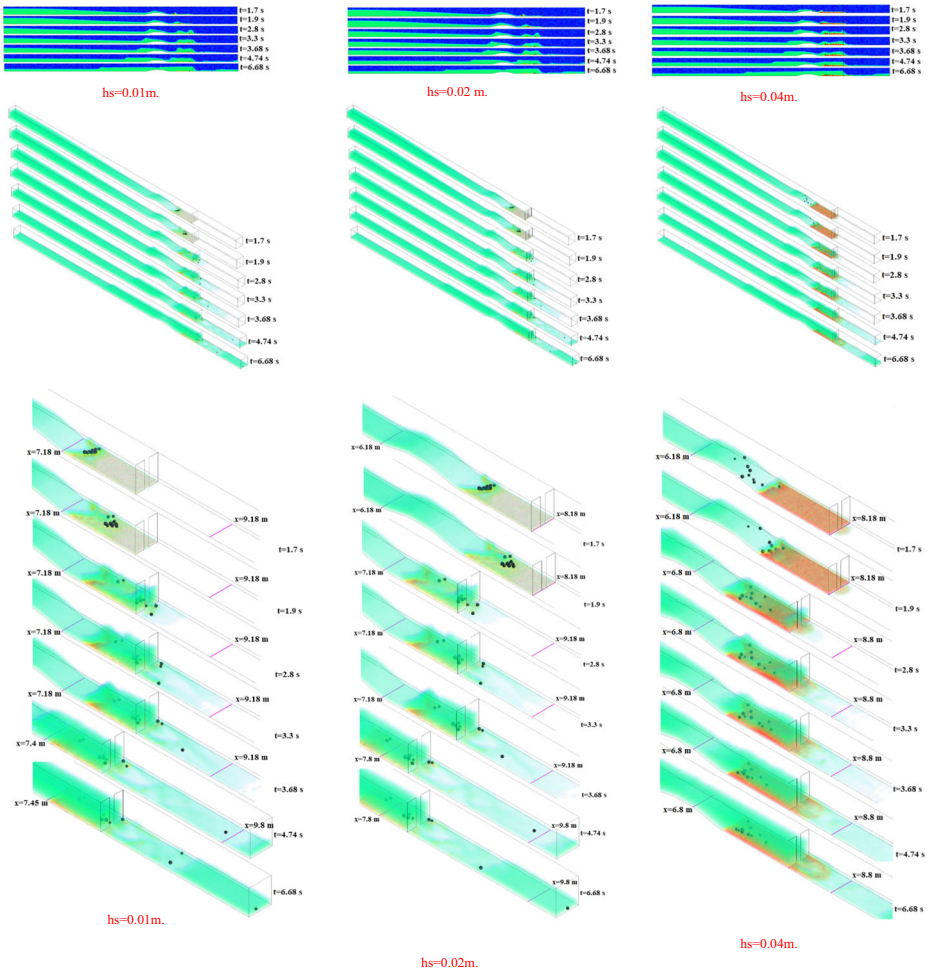

Fig. 10 The 2D-dimensional and 3D-dimensional change in the water interface during the dam break for various times (t = 1.7 s, t = 1.9 s, t = 2.8 s, t = 3.3 s, t = 3.68 s, t = 4.74 s, t = 6.68 s) at different sediment heights (hs = 0.01 m, 0.02 m, 0.04 m)

On the whole, it can be seen from the obtained results that the observed flood wave differs from the typical dam destruction waves above the stationary layers and without taking particles into account, showing that the very presence of the moving layer and macroscopic particles significantly affects the transport of the water flow. The results showed that the flow of the dam break over the moving layer is much softer than the flow of the dam break over a fixed rigid layer. This is due to the fact that the transfer process of the lower layer reduces the energy of the flow with particles. Thus, the presence of a movable layer increased the flow area and, therefore, decreased the flow rate with particles.

Also from the obtained data, it can be noted that in the presence of a mixture of water, macroscopic particles and deposition, there are some time shifts compared to the numerical results without particles and deposition. So at the control points (G5A, GC) in front of

the dam with the hole, it can be observed that mixtures with macroscopic particles and deposits reach faster than without particles and sediment. While at the control point (G8A) the opposite picture is observed. This time shift can be explained by the fact that the mixture consisting of water, macroscopic particles and sediment mixes up, and having passed the heterogeneous terrain, collides with a second obstacle, a dam with a hole, and since the whole mixed mixture cannot pass this hole faster than without a mixture, since this mixture with macroscopic particles and deposits creates additional interference, which leads to the appearance of time shifts.

From Fig. 10, it is possible to clearly trace the behavior of water taking into account particles, so at a time t = 1.7 s the water passes through an inhomogeneous terrain and covers it completely, mixes up with the moving layer by sediment, but still does not encounter an obstacle, a dam with a hole. But even at t = 1.9 s, it could be observed that the water passed through the heterogeneous terrain with a mixture of particles and sediment reaches the dam with the hole and the first collision occurs, however, it must be taken into account that the particles still do not reach the dam with the hole. And at t = 2.8 s, it could be observed that after a collision with the dam with the hole, the reverse flow occurs and the first particles collide against the dam with the hole. And after t = 3.68 s, the reverse flow collides with the flow that goes forward, while the reverse flow practically did not affect the particle propagation. It can also be noticed that, in general, the movement, distribution of particles and mixing with the mixture occurs in a heap when passing through an inhomogeneous terrain and for some time gets stuck when passing through a dam with a hole, since the whole heap of macroscopic particles and the mixture together with water cannot pass at the same time, and the passage is carried out portionwise and the full passage ends after t = 4.74 s.

In general, the obtained results indicate a good agreement between the data from the computation and data from the experiment, both in modeling changes in water levels and changes in soil levels and the propagation of macroscopic particles.

6 Conclusion

The proposed model has been used for numerical modeling of floods during dam destruction over natural rivers with complex channel topography. A well-balanced property between phases has been achieved by the VOF method. To describe this process, a mathematical model was used, which is based on the Navier-Stokes equation, the equation for the phase was used to describe the interface motion. On top of that the DPM and MPM models have been used to describe the particle motion, and for modeling deposition, the effective viscosity was calculated using the model for non-Newtonian fluid.

Verifications of this model were made by comparing with extensive measurement test data and other computational modeling data. Reliability and accuracy of the model are demonstrated in several test cases. Based on the calculated and compared data of various types of cases, it was found that the model is reliable and accurate to simulate floods that are close to reality with inhomogeneous terrain. Predictions using computational modeling illustrated good agreement with the experiment and computational data, in particular, the global behavior of the liquid and the tendency of the change in the height of the water surface were well reproduced. The computational results give great confidence in the effectiveness of the method.

Taking into account the existence of many indeterminations in actual dam destruction, such as partial dam destruction, channel erosion, topography, to implement a realistic dam

breakthrough flow, in this paper, it was considered the use of non-Newtonian and Newtonian models for modeling waves caused by dam destruction over a moving layer for terrain that is close to real case terrain, which can be carried by an unsteady turbulent flow. In this case, the lower mobile layer has been considered as a non-Newtonian fluid. In the first moments after the dam break and near the dam, a huge exchange of momentum between water and mobilized sediments is the main driving mechanism of morphological modifications. Significant morphological changes also occur later and further from the dam.

Also in this study, the model was used to analyze particle transport in the lower reaches of the reservoir. It was found that the effect of floods on the downstream dam varies depending on different sediment depths, the moving layer in the lower reservoir. Particle transfer rate was slower in areas where there were large volumes of the moving layer.

Additional problem were also performed, the problem was the water movement through an inhomogeneous terrain and the dam, which had a hole and which taking into account macroscopic particles (stones) and sediments with different heights. Based on the obtained data, it could be established that by moving the free surface taking into account particles and deposition based on the VOF method, it is possible to accurately and efficiently model 3D problems that are close to real situations. In the future, the obtained data from the computation and the estimation of the SST k-ω turbulent model could be used to model 3D problems with real terrain and real coastal contours when dam breaks. And also to determine the flood zone, taking into account the mixture, which consists of macroscopic particles (stones) and moving sediment, as well as the time of flooding of a certain area, which in the future will make it possible to efficiently and accurately evacuate people from dangerous zones when dam break.

It is should be noted that several limitations exist in this study. The first limitation is the computational grid size and in the number of particles with different sizes: the computer resources restricted in the computational grid size, while very large grid and a lot of particles is needed to simulate accurately, but now it is not achievable, because it was limited by computer resource. The second limitation of this study is the complexity of implementing and analyzing measurement studies at the water surface movement with macroscopic particles on movable beds for heterogeneous terrain (material of particles, sizes, shape, environmental factors). The third limitation is that the shapes of the particles were taken as a sphere, but it should be noticed that in reality the shape of the particle is not the correct shape (uniform shape of particles). The results of this study can be used for real dams with heterogeneous terrain and for environmental protection purposes.

Acknowledgements This work is supported by grant from the Ministry of education and science of the Republic of Kazakhstan (AP05132770).

Compliance with Ethical Standards

Conflict of Interest The authors declare that there is no conflict of interests regarding the publication of this paper.

References

Amicarelli A, Kocak B, Sibilla S, Grabe J (2017) A 3D smoothed particle hydrodynamics model for erosional dam-break floods. International Journal of Computational Fluid Dynamics 31(10):413–434. https://doi.org/10.1080/10618562.2017.1422731

Ancey C, Cochard S (2009) The dam-break problem for Herschel-Bulkley viscoplastic fluids down steep flumes. J Non-Newtonian Fluid Mech 158(1–3):18–35. https://doi.org/10.1016/j.jnnfm.2008.08.008
Ancey C, Andreini N, Epely-Chauvin G (2013) The dam-break problem for concentrated suspensions of neutrally buoyant particles. J Fluid Mech 724:95–122. https://doi.org/10.1017/jfm.2013.154
Andreini N (2012) Dam break of Newtonian fluids and granular suspensions: internal dynamics measurements, Ph.D. thesis, École Polytechnique Fédérale de Lausanne
Balmforth N, Kerswell R (2005) Granular collapse in two dimensions. J Fluid Mech 538:399–428. https://doi.org/10.1017/S0022112005005537
Boroomand MR, Salehi-Neyshaboury AA, Aghajanloo K (2007) Numerical simulation of sediment transport and scouring by an offset jet. Canadian Journal of Civil Eng 34:1267–1275. https://doi.org/10.1139/l07-050
Chambon G, Ghemmour A, Laigle D (2009) Gravity-driven surges of a viscoplastic fluid: an experimental study. J Non-Newtonian Fluid Mech 158(1–3):54–62. https://doi.org/10.1016/j.jnnfm.2008.08.006
Chara Z, Kysela B (2018) Application of macroscopic particle model to simulate motion of large particles. AIP Conf Proc 1978:030031. https://doi.org/10.1063/1.5043681
Coussot P (1995) Structural similarity and transition from Newtonian to non-Newtonian behavior for clay-water suspensions. Phys Rev Lett 74(20):3971–3974. https://doi.org/10.1103/PhysRevLett.74.3971
Crespo AJ, Gymez-Gesteira M, Dalrymple RA (2008) Modeling dam break behavior over a wet bed by a SPH technique. J Waterw Port Coast Ocean Eng 134(6):313–320. https://doi.org/10.1061/(ASCE)0733-950X(2008)134:6(313)
Di Cristo C, Leopardi A, Greco M (2010) Modeling dam break granular flow. Proceedings of international conference of river flow, pp 895–901
Ferrari A, Fraccarollo L, Dumbser M, Toro EF, Armanini A (2010) Three-dimensional flow evolution after a dam break. J Fluid Mech 663:456–477. https://doi.org/10.1017/S0022112010003599
Fondelli T, Andreini A, Facchini B (2015) Numerical simulation of dam-break problem using an adaptive meshing approach. Energy Procedia 82:309–315. https://doi.org/10.1016/j.egypro.2015.12.038
Fraccarollo L, Toro EF (1995) Experimental and numerical assessment of the shallow water model for two-dimensional dam-break type problems. J Hydraul Res 33(6):843–864. https://doi.org/10.1080/00221689509498555
Gotoh H, Fredsøe J (2000) Lagrangian two-phase flow model of the settling behavior of fine sediment dumped into water. In: Proceedings of the ICCE, Sydney, Australia, pp 3906–3919
Haltas I, Elci S, Tayfur G (2016a) Numerical simulation of flood wave propagation in two-dimensions in densely populated urban areas due to dam break. Water Resour Manag 30(15):5699–5721. https://doi.org/10.1007/s11269-016-1344-4
Haltas I, Tayfur G, Elci S (2016b) Two-dimensional numerical modeling of flood wave propagation in an urban area due to Urkmez dam-break, Izmir, Turkey. Nat Hazards 81(3):2103–2119. https://doi.org/10.1007/s11069-016-2175-6
Hirt CW, Nichols BD (1981) Volume of fluid (VOF) method for the dynamics of free boundaries. J Comput Phys 39:201. https://doi.org/10.1016/0021-9991(81)90145-5
Hogg AJ, Pritchard D (2004) The effects of drag on dam-break and other shallow inertial flows. J Fluid Mech 501:179–212. https://doi.org/10.1017/S0022112003007468
Hogg AJ, Woods AW (2001) The transition from inertia to drag-dominated motion of turbulent gravity currents. J Fluid Mech 449:201–224. https://doi.org/10.1017/S0022112001006292
Hosseinzadeh-Tabrizi SA, Ghaeini-Hessaroeyeh M (2017) Application of bed load formulations for dam failure and overtopping. Civ Eng J 3(10):997–1007
Issa RI (1986) Solution of the implicitly discretized fluid flow equations by operator splitting. J Comput Phys 62(1):40–65. https://doi.org/10.1016/0021-9991(86)90099-9
Issakhov A, Imanberdiyeva M (2019) Numerical simulation of the movement of water surface of dam break flow by VOF methods for various obstacles. Int J Heat Mass Transf 136:1030–1051. https://doi.org/10.1016/j.ijheatmasstransfer.2019.03.034
Issakhov A, Zhandaulet Y (2020) Numerical study of dam break waves on movable beds for complex terrain by volume of fluid method. Water Resour Manag 34(2):463–480. https://doi.org/10.1007/s11269-019-02426-1
Issakhov A, Zhandaulet Y, Nogaeva A (2018) Numerical simulation of dam break flow for various forms of the obstacle by VOF method. Int J Multiphase Flow 109:191–206. https://doi.org/10.1016/j.ijmultiphaseflow.2018.08.003
Janosi IM, Jan D, Szabo KG, Tel T (2004) Turbulent drag reduction in dam break flows. Exp Fluids 37:219–229. https://doi.org/10.1007/s00348-004-0804-4
Kleefsman KMT, Fekken G, Veldman AEP, Iwanowski B, Buchner B (2005) A volume-of-fluid based simulation method for wave impact problems. J Comput Phys 206(1):363–393. https://doi.org/10.1016/j.jcp.2004.12.007

Kocaman S (2007) Experimental and theoretical investigation of dam-break problem. Ph.D. dissertation, University of Cukurova, Adana, Turkey
Larocque LA, Imran J, Chaudhry MH (2013) 3D numerical simulation of partial breach dam-break flow using the LES and k-e turbulence models. J Hydraul Res 51(2):145–157. https://doi.org/10.1080/00221686.2012.734862
Lauber G, Hager WH (1998) Experiments to dam break wave: horizontal channel. J Hydraul Res 36(3):291–307. https://doi.org/10.1080/00221689809498620
Li X, Zhao J (2018) Dam-break of mixtures consisting of non-Newtonian liquids and granular particles. Powder Technol 338:493–505. https://doi.org/10.1016/j.powtec.2018.07.021
Lin S, Chen Y (2013) A pressure correction-volume of fluid method for simulations of fluid-particle interaction and impact problems. Int J Multiphase Flow 49:31–48. https://doi.org/10.1016/j.ijmultiphaseflow.2012.09.003
Lube G, Huppert HE, Sparks RSJ, Freundt A (2005) Collapses of two-dimensional granular columns. Phys Rev E 72(4):041301. https://doi.org/10.1103/PhysRevE.72.041301
Luchini TJF, Sommerlot SJ, Loos AC Effects of disordered touching particles on unidirectional fiber reinforcement permeability. 20th international conference on composite materials, Copenhagen, 19–24 July 2015
Marsooli R, Wu W (2014) 3-D finite-volume model of dam-break flow over uneven beds based on VOF method. Adv Water Resour 70:104–117. https://doi.org/10.1016/j.advwatres.2014.04.020
Minussi RB, Maciel GdF (2012) Numerical experimental comparison of dam break flows with non-Newtonian fluids. J Braz Soc Mech Sci Eng 34(2):167–178. https://doi.org/10.1590/S1678-58782012000200008
Movahedi A, Kavianpour MR, Aminoroayaie Yamini O (2018) Evaluation and modeling scouring and sedimentation around downstream of large dams. Environ Earth Sci 77:320–317. https://doi.org/10.1007/s12665-018-7487-2
Ozmen-Cagatay H, Kocaman S (2011) Dam-break flow in the presence of obstacle: experiment and CFD simulation. Eng Appl Comp Fluid 5(4):541–552. https://doi.org/10.1080/19942060.2011.11015393
Park KM, Yoon HS, Kim MI (2018) CFD-DEM based numerical simulation of liquid-gas particle mixture flow in dam break. Commun Nonlinear Sci Numer Simul 59:105–121. https://doi.org/10.1016/j.cnsns.2017.11.010
Piau J-M (2006) Consistometry slump and spreading tests: practical comments. J Non-Newtonian Fluid Mech 135(2–3):177–178. https://doi.org/10.1016/j.jnnfm.2006.02.001
Pitman EB, Le L (2005) A two-fluid model for avalanche and debris flows. Philos Trans R Soc Lond A 363(1832):1573–1601. https://doi.org/10.1098/rsta.2005.1596
Pontillo M (2010) Trasporto ed "entrainment" di sedimenti in alvei mobile. PhD diss., Universita degli studi di Napoli Federico II
Ran Q, Tong J, Shao S, Fu X, Xu Y (2015) Incompressible SPH scour model for movable bed dam break flows. Adv Water Resour 82:39–50. https://doi.org/10.1016/j.advwatres.2015.04.009
Roussel N, Coussot P (2005) "Fifty-cent rheometer" for yield stress measurements: from slump to spreading flow. J Rheol 49(3):705–718. https://doi.org/10.1122/1.1879041
Saak AW, Jennings HM, Shah SP (2004) A generalized approach for the determination of yield stress by slump and slump flow. Cem Concr Res 34(3):363–371. https://doi.org/10.1016/j.cemconres.2003.08.005
Saramito P, Smutek C, Cordonnier B (2013) Numerical modeling of shallow non-Newtonian flows: part I. the 1D horizontal dam break problem revisited. Int J Numer Anal Model Ser B 4(3):283–298
Spinewine B (2010) Two-layer flow behavior and the effects of granular dilatancy in dam-break induced sheet-flow. PhD diss., Faculte des sciences appliquees, Universite catholique de Louvain
Spinewine B, Zech Y (2007) Small-scale laboratory dam-break waves on movable beds. J Hydraul Res 45(sup1):73–86. https://doi.org/10.1080/00221686.2007.9521834
Wadnerkar D, Agrawal M, Tade MO, Pareek V (2016) Hydrodynamics of macroscopic particles in slurry suspensions. Asia Pac J Chem Eng 11(3):467–479. https://doi.org/10.1002/apj.1975
Wang JS, Ni HG, He YS (2000) Finite-difference TVD scheme for computation of dam break problems. J Hydraul Eng 126(4):253–262. https://doi.org/10.1061/(ASCE)0733-9429(2000)126:4(253)
Wang C, Wang Y, Peng C, Meng X (2016) Smoothed particle hydrodynamics simulation of water-soil mixture flows. J Hydraul Eng 142(10):04016032. https://doi.org/10.1061/(ASCE)HY.1943-7900.0001163
Ward T, Wey C, Glidden R, Hosoi A, Bertozzi A (2009) Experimental study of gravitation effects in the flow of a particle-laden thin film on an inclined plane. Phys. Fluids 21(8). https://doi.org/10.1063/1.3208076
Xu X (2016) An improved SPH approach for simulating 3D dam-break with breaking waves. Comput Methods Appl Mech Eng 311:723–742. https://doi.org/10.1016/j.cma.2016.09.002